Lipoplexes Formed by DNA and Ferrocenyl Lipids: Effect of Lipid Oxidation State on Size, Internal Dynamics, and ζ-Potential

Melissa E. Hays,* Christopher M. Jewell,* Yukishige Kondo,† David M. Lynn,* and Nicholas L. Abbott*
*Department of Chemical and Biological Engineering, University of Wisconsin-Madison, Madison, Wisconsin; and †Department of Industrial Chemistry, Tokyo University of Science, Tokyo, Japan

ABSTRACT The effect of lipid oxidation state on the physical properties of complexes formed by plasmid DNA and the redox-active lipid bis-(11-ferrocenylundecyl)dimethylammonium bromide (BFDMA) is reported. With increasing concentration of BFDMA, the hydrodynamic sizes of complexes formed by BFDMA and DNA (in the presence of 1 mM Li_2SO_4) pass through a maximum and the ζ-potential changes monotonically from –40 mV to +40 mV. In contrast, complexes formed by oxidized BFDMA and DNA exhibit a minimum in size and maintain a negative ζ-potential with increasing concentration of BFDMA. Angle-dependent dynamic light scattering measurements also reveal the presence of relaxation processes within complexes formed by DNA and oxidized BFDMA that are absent for complexes formed by DNA and reduced BFDMA. These results, when combined, reveal that the amphiphilic nature of reduced BFDMA leads to lipoplexes with physical properties resembling those formed by classical cationic lipids, whereas the interaction of oxidized BFDMA with DNA is similar to that of nonamphiphilic cationic molecules bearing multiple charges (e.g., spermidine). In particular, the negative ζ-potential and measurable presence of DNA chain dynamics within complexes formed by oxidized BFDMA and DNA indicate that these complexes are loosely packed with excess charge due to DNA in their outer regions. These results, when combined with additional measurements performed in OptiMEM reduced-serum cell culture medium, lead to the proposition that the strong dependence of transfection efficiency on the oxidation state of BFDMA, as reported previously, is largely a reflection of the substantial change in the ζ-potentials of these complexes with changes in the oxidation state of BFDMA.

INTRODUCTION

The ability of cationic lipids to form physical complexes with DNA and promote the delivery of DNA to cells is well known (1,2). Several past studies have reported cationic lipids with structures designed to optimize the efficiency of transfection, minimize toxicity, and target the time or location of the delivery of DNA (3–15). In past studies aimed at addressing the latter goals, we have shown that the redox-active cationic lipid bis-(11-ferrocenylundecyl)dimethylammonium bromide (BFDMA, Fig. 1) (16–18) is capable of transfecting cells in a manner that is strongly dependent upon the oxidation state of the lipid (19,20). Reduced BFDMA was found to promote efficient transfection of cells, whereas oxidized BFDMA, formed by electrochemical oxidation of the ferrocene groups of the lipid to positively-charged ferrocenium ions, did not lead to high levels of transgene expression. This dependence of transfection efficiency on the oxidation state of BFDMA suggests the basis of an approach that could lead to novel gene delivery systems that permit spatial and temporal control of DNA delivery by chemical and/or electrochemical manipulation of the oxidation state of BFDMA. In this article, we report a detailed investigation of the physical properties of complexes formed by DNA and either reduced or oxidized BFDMA to provide insight into possible physical mechanisms by which the oxidation state of BFDMA may impact cell transfection.

Transfection of cells using DNA-lipid assemblies is a complex process involving multiple steps, culminating in the expression of a functional protein encoded by DNA. The first step in this process is transfer of the lipid-DNA complex, or lipoplex, across the outer membrane of the cell. Past studies have identified a number of physical properties of lipoplexes that are important in influencing the passage of DNA across cell membranes, including aggregate size, ζ-potential, and microstructure (4,5,7,21–26). Although the mechanisms by which these physical properties influence cell transfection are the subject of ongoing research, it is now generally accepted that transport of lipoplexes by endocytosis is size-dependent, with optimal sizes (diameters) ranging from ~70 nm to ~200 nm (23,27,28). Evidence also exists that lipoplexes that are too large to be internalized by endocytosis (e.g., from 500 nm to >1 μm) may be transported across cell membranes by other mechanisms, including direct fusion with the cell membrane (29). The ζ-potentials of lipoplexes have also been identified as a physical parameter that can play an important role in promoting transfection. Efficient, nonspecific transport of lipoplexes into cells often correlates with positive ζ-potentials, presumably resulting from electrostatic interactions that occur between the positively charged lipoplexes and negatively charged cell membranes (22,25,30).

The physical properties of complexes formed between cationic lipids and DNA are, in general, strongly dependent upon the amphiphilicity of the cationic molecule (21,27).

Submitted February 24, 2007, and accepted for publication May 23, 2007.

Address reprint requests to D. M. Lynn, Tel.: 608-262-1086; E-mail: dlynn@engr.wisc.edu; or N. L. Abbott, Tel.: 608-265-5278; E-mail: abbott@engr.wisc.edu.

Editor: Petra Schwille.

0006-3495/07/12/4414/11 $2.00

doi: 10.1529/biophysj.107.107094

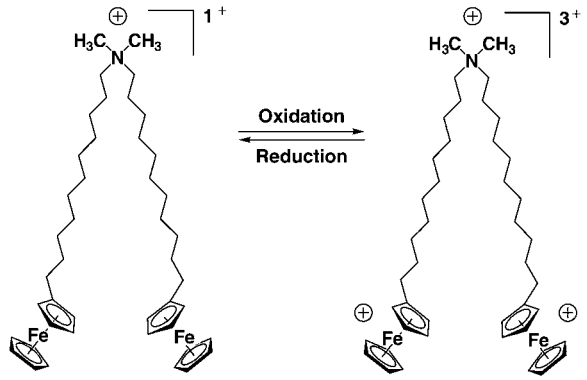

FIGURE 1 Molecular structure of BFDMA.

The study reported in this article was motivated by the observation that the amphiphilic character of BFDMA is perturbed upon oxidation of ferrocene to ferrocenium (16,17). Past studies have reported that reduced BFDMA forms vesicle-like assemblies, whereas oxidized BFDMA does not (16,17). We hypothesized that this redox-induced change in the amphiphilic character of BFDMA would lead to changes in the physical properties of complexes formed by BFDMA and DNA that could be understood in the context of past studies of the interactions of DNA with self-associating and non-self-associating cationic molecules, as discussed below.

When DNA is added to a solution of a cationic lipid that strongly self-associates (e.g., into vesicles), electrostatic interactions between the lipid assemblies and DNA lead to the formation of organized DNA-lipid complexes. These complexes have been demonstrated to possess internal organization, including lamellar (5,31,32), hexagonal (5,7,31), or cubic microstructures (33). The microstructures and physical properties of the DNA-lipid complexes generally depend on the molar charge ratio (CR) of cationic lipid to DNA used to prepare the lipoplexes. The hydrodynamic sizes of many lipoplexes exhibit a characteristic dependence on CR, with maximum sizes observed at CRs of approximately unity. The ζ-potentials of lipoplexes formed from self-associating molecules typically change from negative to positive values with increasing CR, with the change in sign of the ζ-potential also occurring around a CR of unity (4,21–23,25,26,30). In contrast, complexes formed from DNA and cationic species that possess multiple charges but do not self-associate (such as spermidine $(H_3N^+(CH_2)_3NH_2^+(CH_2)_4 - NH_3^+)$ or $Co(NH_3)_6^{3+}$) exhibit a minimum in size with increasing CR (34–41). These nonamphiphilic cationic species tend to form large aggregates at high CRs (e.g., aggregates >1 μm are formed at CRs $\sim$50 or higher) (34,42,43). Whereas the ζ-potentials of lipoplexes formed from cationic lipids change sign with increasing CR, the ζ-potentials of complexes formed by DNA and spermidine are negative for CRs ranging from 0.1 to 50 (42,43). We also note in this context that the transfection efficiency of spermidine is, in general, substantially lower than that of many cationic lipids (44,45).

In this study, we characterized complexes formed by plasmid DNA and BFDMA as a function of the concentration and oxidation state of BFDMA by using measurements of dynamic light scattering and ζ-potential. Further insights were obtained by comparing the properties of these complexes formed using BFDMA with those formed using classical cationic lipids and by investigating the effects of added salts. These results, when combined, suggest ways in which the oxidation state of BFDMA in DNA-BFDMA complexes may influence transfection of cells.

MATERIALS AND METHODS

Materials

BFDMA was synthesized as described previously (18). Lithium sulfate monohydrate (Sigma Aldrich, St. Louis, MO), dioctadecyldimethylammonium bromide (DoDAB, Sigma Aldrich) and dioleoylphosphatidylethanolamine (DOPE, Avanti Polar Lipids, Alabaster, AL) were used as received. Plasmid DNA encoding enhanced green fluorescent protein (pEGFP-N1 (4.7 kb), >95% supercoiled) was obtained from the Waisman Clinical Biomanufacturing Facility at the University of Wisconsin-Madison. OptiMEM cell culture medium (#11058-021) was purchased from Gibco (Invitrogen, Carlsbad, CA).

Methods

Sample preparation

Reduced BFDMA was electrochemically oxidized at 0.5V relative to a silver|silver chloride reference electrode, and solutions of BFDMA and DNA were prepared as described previously (19,20). Unless otherwise stated, all solutions contained 2.4 μg/mL DNA (7.3 μM concentration of PO_4^- in DNA). The concentrations of BFDMA used in this study were 2, 6, 8, 10, 20, 60, and 100 μM. The solutions containing BFDMA and DNA were placed in a thermostated water bath set at 37°C for at least 1 h before light scattering or ζ-potential measurements. Unless otherwise stated, all measurements were performed in 1 mM Li_2SO_4 (pH 5) because this electrolyte was necessary for electrochemical control of the oxidation state of the BFDMA in past studies (19,20).

Aqueous dispersions of the lipids DoDAB and DOPE were prepared as described previously (46). Briefly, DoDAB and DOPE were mixed at a 1:1 molar ratio in chloroform and then dried under a flowing stream of argon overnight. The mixed lipid film was reconstituted in water and extruded 29 times through a pair of 0.2 μm polycarbonate membranes from Whatman (Gardena, CA) using a miniextruder from Avanti Polar Lipids (Alabaster, AL). These lipids were combined with DNA as described for the BFDMA system (19,20).

Dynamic light scattering measurements

A 100-mW, 532-nm laser (Compass 315M-100, Coherent, Santa Clara, CA) illuminated a temperature-controlled glass cell at 37°C that was filled with a refractive-index matching fluid (decahydronaphthalene, Fisher Scientific, Pittsburgh, PA). The scattering of light was measured at angles of 110°, 90°, 75°, 60°, and 45°, unless stated otherwise. The autocorrelation functions (ACFs) were obtained using a BI-9000AT digital autocorrelator (Brookhaven Instruments, Holtsville, NY).

Analysis of autocorrelation functions

The ACFs were analyzed using an intensity-based CONTIN (47–49) analysis to yield a distribution of relaxation times. For center-of-mass (CM) diffusion of an aggregate in solution, the CM diffusion coefficient, D, is related to the relaxation time, τ, by

$$D = \frac{1}{\tau \cdot q^2}, \tag{1}$$

where q is the magnitude of the scattering vector and related to the scattering angle, θ, by

$$q = \frac{4\pi n}{\lambda}\sin\left(\frac{\theta}{2}\right). \tag{2}$$

In Eq. 2, n is the refractive index and λ is the wavelength. The hydrodynamic diameter of an aggregate was calculated from D using the Stokes-Einstein relationship (50).

We interpreted some light scattering data using a model of the ACF that comprises two relaxation modes characterized by τ_f and τ_s, referred to as the fast and slow relaxation times, respectively. The form of the corresponding ACF for the electric field of the scattered light $g^1(q,\tau)$ is

$$g^1(q,\tau) = A_f \exp\left(-\frac{\tau}{\tau_f}\right) + A_s \exp\left[\left(-\frac{\tau}{\tau_{se}}\right)^{\beta}\right], \tag{3}$$

where $A_f + A_s = 1$. The stretching parameter, β, characterizes the width of the distribution of slow relaxation times. This model has been used in past studies of polymer-surfactant systems (51–53). The fast relaxation time is typically related to CM diffusion. The slow relaxation time, τ_s, calculated from τ_{se} in Eq. 3 (51–53), has been associated with several different phenomena, including viscous flow relaxations, dissociations of polymeric clusters, and dynamics of individual polymer chains (54,55).

ζ-potential measurements

Measurements of ζ-potential were performed using a Zetasizer 3000HS (Malvern Instruments, Worcestershire, UK). The measurements were performed at ambient temperature using an applied voltage of 150 V. The Henry equation was used to calculate ζ-potentials from measurements of electrophoretic mobility (56). In this calculation, we assumed the viscosity of the solution to be the same as water.

RESULTS

Dynamic light scattering of complexes of BFDMA and DNA

We performed dynamic light scattering (DLS) measurements to characterize complexes formed from DNA and BFDMA in terms of 1), center-of-mass (CM) diffusion and, thus, hydrodynamic size; and 2), relaxation processes related to the dynamics of DNA chains within the complexes. The autocorrelation functions (ACFs) of DNA in the absence and presence of reduced BFDMA are shown in Fig. 2 *a*. We note that for the data presented in Fig. 2 *a*, the concentration of DNA in the absence of BFDMA was increased to 66 μg/mL (200 μM PO_4^-, as compared to 7.3 μM PO_4^- for all other experiments) to obtain intensities of scattered light that were sufficient for accurate measurements of the ACF. Fig. 2 *b* shows results obtained using DNA and oxidized BFDMA. For the solutions containing DNA and reduced BFDMA, we measured the relaxation times to increase with addition of BFDMA up to a concentration of 20 μM and then decrease with further addition of reduced BFDMA (Fig. 2 *a*). In contrast, the relaxation times measured using solutions of oxidized BFDMA decreased with increasing concentration of oxidized BFDMA up to a concentration of 20 μM and then increased rapidly with further addition of reduced BFDMA (Fig. 2 *b*). These results reveal that qualitative differences in the ACFs are generated by changes in the oxidation state of the BFDMA. Below we quantitatively analyze the ACFs shown in Fig. 2.

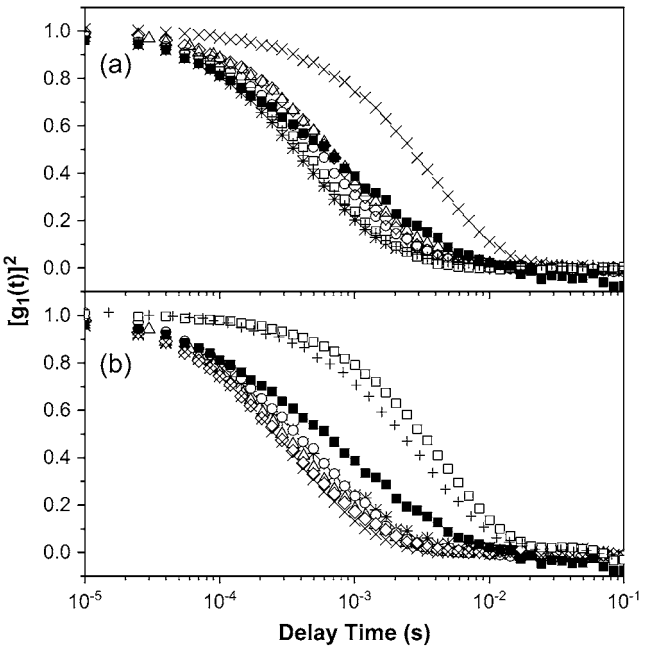

FIGURE 2 Autocorrelation functions (ACFs) obtained using aqueous solutions of DNA and mixtures of DNA and BFDMA at a scattering angle of 90° and temperature of 37°C. (*a*) ACFs corresponding to solutions of DNA and reduced BFDMA. (*b*) ACFs corresponding to solutions of DNA and oxidized BFDMA. The symbols correspond to DNA alone (■), and solutions of DNA and BFDMA at 2 μM (*), 6 μM (○), 8 μM (Δ), 10 μM (◇), 20 μM (×), 60 μM (□), and 100 μM (+). Concentrations of DNA used in each experiment are as noted in the text.

Before it is possible to interpret the ACFs in Fig. 2 in terms of size, it is necessary to determine whether the ACFs arise solely from center-of-mass (CM) diffusion of the complexes. Previous light scattering studies have reported that for relatively short DNA fragments (<2500 bp), both internal motions of the DNA chains and translational diffusion can contribute to the scattering measured at angles higher than 57° (57,58). Most light scattering studies of lipoplexes prepared using plasmid DNA have been measured only at 90° (26,30,59–63). As discussed below, it is not possible to interpret ACFs solely in terms of CM diffusion if the ACFs are measured at only one angle.

Light scattering of complexes formed by reduced BFDMA and DNA

To determine whether dynamic processes within complexes of DNA and BFDMA contributed to the ACFs shown in Fig. 2, we performed DLS measurements using solutions of DNA and BFDMA at concentrations ranging from 2 μM to 100 μM in 1 mM Li_2SO_4 at multiple scattering angles (105°, 90°, 75°, 60°, and 45°). In cases where CM diffusion is the only contributor to the ACF, the relaxation times are inversely proportional to q^2 (Eq. 1), where q is the magnitude of the scattering vector. As noted above, because past studies have indicated that relaxation processes associated with DNA chain dynamics can, under some conditions, contribute to the ACFs in dynamic light scattering experiments (57,58), we first rescaled the ACFs obtained using solutions of DNA only with q^2 (Fig. 3 *a*). Inspection of Fig. 3 *a* reveals that the rescaled ACFs do not superimpose on each other, indicating that CM diffusion is not the only contribution to the ACFs and, therefore, that the ACFs may not be interpreted solely in terms of CM diffusion (see below for further details) (57,58). In contrast, the rescaled ACFs obtained using solutions of DNA and 2–100 μM reduced BFDMA do superimpose on each other, indicating that internal motions of the DNA chains within the lipoplexes do not contribute to the ACFs (see Fig. 3 *b* for a representative example of ACFs of lipoplexes prepared using 10 μM reduced BFDMA). We conclude that the addition of reduced BFDMA to a solution of DNA eliminates the contributions of the DNA chain dynamics to the ACF, consistent with a physical situation in which the DNA is constrained within the structured interior of a lipoplex (see below) (4,5,24).

The results described above permit the interpretation of the ACFs obtained for lipoplexes prepared using reduced BFDMA in terms of CM diffusion. The hydrodynamic sizes of the lipoplexes formed using reduced BFDMA were calculated from the data presented in Fig. 4 *a* by using an intensity-based CONTIN analysis. The figure shows the hydrodynamic diameters of the lipoplexes as a function of the concentration of BFDMA (Fig. 4 *a*) and CR (Fig. 4 *b*). At low concentrations (2–10 μM) and high concentrations (60–100 μM) of reduced BFDMA, we observed lipoplexes with sizes ranging in diameter from 400 nm to 700 nm. Lipoplexes of DNA and 20 μM reduced BFDMA (corresponding to a CR of 2.75) were calculated to be more than 2 μm in diameter, revealing a well-defined maximum in size as a function of concentration of reduced BFDMA.

The dependence of the sizes of the reduced BFDMA lipoplexes on CR described above is similar to that observed for lipoplexes prepared using conventional vesicle-forming cationic lipids such as a 1:1 molar mixture of dioctadecyldimethylammonium bromide (DoDAB) and dioleoylphosphatidylethanolamine (DOPE; see Fig. 4 *b* and Supplementary Materials). These cationic lipids typically form lipoplexes with a maximum in hydrodynamic size at CRs ranging from 1 to 3 (4,21,24,26), similar to reduced BFDMA. We also note that the ACFs of lipoplexes formed using DoDAB/DOPE obtained at multiple angles did not reveal evidence of internal DNA chain dynamics, as was reported above for the reduced BFDMA lipoplexes (see Supplementary Materials). This result is consistent with a physical situation in which the internal organization of the lipoplex hinders DNA chain dynamics to an extent that they are not apparent in the ACFs.

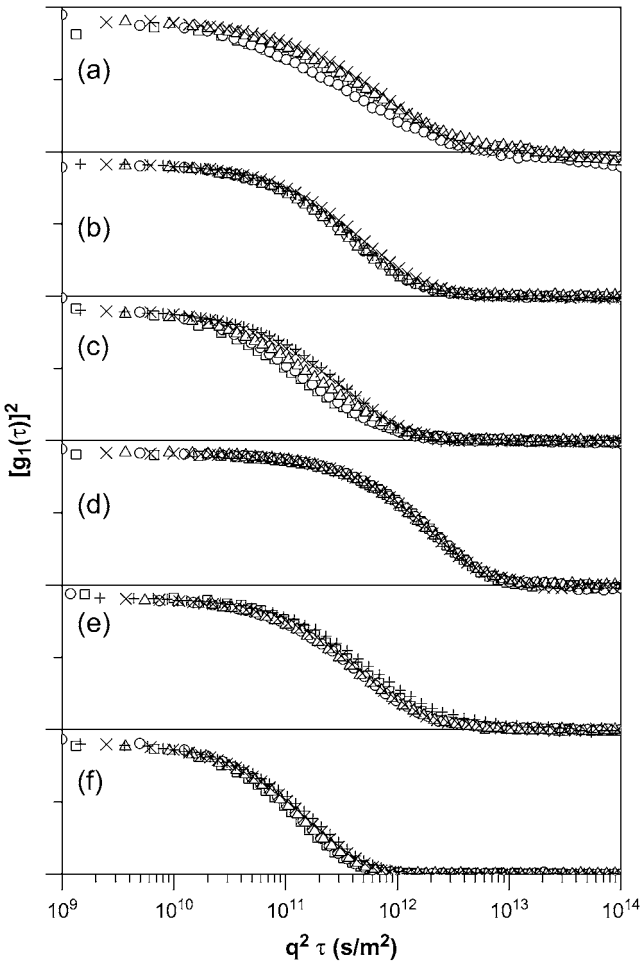

FIGURE 3 Autocorrelation functions of solutions measured at 37°C and scattering angles of 110° (□), 90° (○), 75° (Δ), 60° (×), and 45° (+). The ACFs for each experiment have been offset for clarity and correspond to (*a*) DNA alone, (*b*) DNA and 10-μM reduced BFDMA, (*c*) DNA and 10-μM oxidized BFDMA, (*d*) DNA and 60-μM oxidized BFDMA, (*e*) DNA and 10-μM reduced BFDMA, and (*f*) DNA and 10-μM oxidized BFDMA. Samples in panels *a–d* were prepared in 1 mM Li_2SO_4 and samples in panels *e* and *f* were prepared in OptiMEM. Concentrations of DNA used in each experiment are as noted in the text.

Light scattering of complexes formed by oxidized BFDMA and DNA

To explore the angle-dependent measurements of the ACFs of solutions containing DNA and oxidized BFDMA, we return to Fig. 3. We observed that the behavior of these

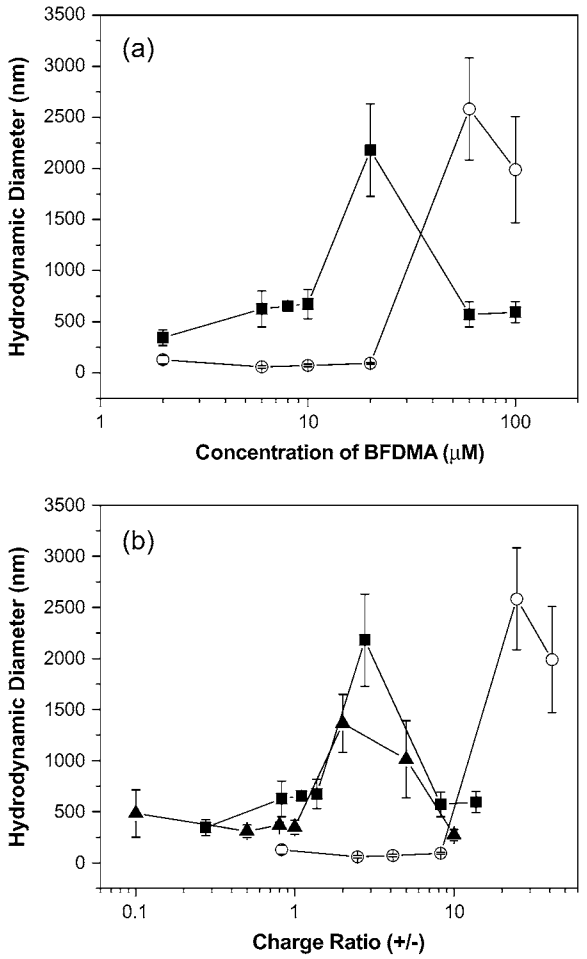

FIGURE 4 Hydrodynamic diameters of lipoplexes formed using solutions of DNA and lipid (BFDMA or DoDAB/DOPE) in 1 mM Li_2SO_4. (*a*) Plot of hydrodynamic diameters as a function of the concentration of BFDMA and (*b*) plot of hydrodynamic diameters as a function of CR. The symbols correspond to the sizes of complexes prepared using DNA and reduced BFDMA (■), oxidized BFDMA (○), and DoDAB/DOPE (1:1) (▲).

complexes contrasts with that of lipoplexes prepared using reduced BFDMA (Fig. 3 *b*). For example, Fig. 3 *c* demonstrates that the rescaled ACFs obtained using solutions of DNA and 10 μM oxidized BFDMA do not superimpose on each other, but instead contain relaxation times that shift to longer delay times as the scattering angle decreases from 110° to 45°. The ACFs of all DNA complexes prepared using oxidized BFDMA at concentrations varying from 2 μM to 20 μM did not superimpose on each other, similar to the data shown in Fig. 3 *c* (data not shown). This behavior suggests that CM diffusion is not the only contribution to the ACFs of the solutions of DNA and oxidized BFDMA and that these ACFs may not be interpreted solely in terms of hydrodynamic size. It also suggests that the DNA in solutions of 2–20 μM oxidized BFDMA possesses conformational degrees of freedom that are greater than those in solutions of DNA and reduced BFDMA. When the concentration of oxidized BFDMA was increased beyond 20 μM, we observed the rescaled ACFs of complexes to overlap (e.g., Fig. 3 *d* corresponds to complexes formed using 60-μM oxidized BFDMA), suggesting that CM diffusion dominates the relaxation processes giving rise to these ACFs.

To interpret the ACFs that do not arise from CM diffusion only, it is necessary to identify the subset of relaxation processes in the ACF that are due to CM diffusion. For the solution of DNA alone, we used an intensity-based CONTIN analysis to identify two peaks in the distribution of relaxation times (see Supplementary Materials). By plotting $\log(1/\tau)$ versus $\log(q)$ for each peak (see Eq. 1), we determined that the faster relaxation process had a slope of -2.01 ± 0.44 (indicating CM diffusion). Therefore, we were able to calculate the hydrodynamic diameter of the plasmid DNA to be 105 ± 23 nm, which is similar to that reported previously (30,57–59). The slow relaxation time was ~4 ms at a scattering angle of 90°, which is similar in magnitude to that reported in previous studies of DNA (57,58). In contrast, a CONTIN analysis of the ACFs of complexes formed from DNA and 2–20 μM oxidized BFDMA (shown in Fig. 3 *b*) did not resolve the distribution of relaxation times into two peaks (as described for DNA only). Instead, only a single, very broad peak was observed. However, by using a double-stretched exponential model (in Eq. 3), which has been used previously to fit the ACFs of polymer-amphiphile mixtures with multiple relaxation processes (51,53), we were able to identify two relaxation times. Using this methodology, we determined that the fast relaxation times shown in Table 1 correspond to CM diffusion for all samples containing 2–20 μM BFDMA, with the exception of the sample containing 8 μM BFDMA. The slow relaxation times, τ_s, in Table 1 are comparable to the slow relaxation times for DNA alone, suggesting that the internal dynamics of the DNA in these complexes are not substantially restricted as compared to free DNA. As mentioned above, the ACFs of solutions of

TABLE 1 Analysis of ACFs of solutions of DNA and oxidized BFDMA

Concentration of oxidized BFDMA (μM)	Hydrodynamic diameter (nm)*	τ_f Angle dependence†	Slow relaxation time, τ_s (ms)‡
2	129 ± 44	2.00 ± 0.64	2.7 ± 0.3
6	58 ± 13	2.15 ± 0.42	2.3 ± 0.4
8	NA	3.04 ± 0.57	NA
10	73 ± 12	2.00 ± 0.30	2.5 ± 0.6
20	94 ± 10	2.12 ± 0.22	1.7 ± 0.4
60	2580 ± 500	2.03 ± 0.04	NA
100	1990 ± 520	1.97 ± 0.14	NA

*A double-stretched exponential was used to calculate the hydrodynamic diameter for solutions of DNA and 2–20 μM oxidized BFDMA and an intensity-based CONTIN analysis was used to calculate the diameter of solutions of DNA and 60–100 μM oxidized BFDMA (see text).

†Dependence of the fast relaxation time on the scattering vector for each solution.

‡Slow relaxation time reported at a scattering angle of 90°.

DNA in the presence of 60–100 μM oxidized BFDMA did not reveal evidence of internal DNA chain dynamics. The hydrodynamic sizes of these complexes were calculated using an intensity-based CONTIN analysis similar to that used in analyses of solutions containing DNA and reduced BFDMA.

The analysis presented above allowed us to calculate the hydrodynamic sizes of complexes formed using oxidized BFDMA and DNA using the ACFs in Fig. 3 *b*. The results presented in Fig. 4 and Table 1 show that complexes prepared at 2 μM oxidized BFDMA are approximately the same size as DNA in the absence of BFDMA (105 $\pm$ 23 nm). The hydrodynamic sizes of the complexes decrease in the presence of 6–20 μM oxidized BFDMA (see Table 1), consistent with the condensation of DNA. A minimum in hydrodynamic size is reached at a concentration of oxidized BFDMA between 6 μM and 10 μM. Complexes prepared from DNA and 60–100 μM oxidized BFDMA were significantly larger ($>$2 μm in diameter) than complexes prepared using 2–20 μM oxidized BFDMA. These observations are similar to those reported previously using cationic molecules with three positive charges that do not self-associate (e.g., spermidine). Spermidine condenses DNA at CRs ranging from $<$1 to $\sim$30, and causes the formation of large ($>$1 μm) aggregates at CRs $>$50 (34–43). We suggest that low concentrations of oxidized BFDMA (2–20 μM, corresponding to CRs 0.825–8.25) promote the condensation of DNA into loosely-packed aggregates that largely preserve the dynamics of the free DNA. This view is supported by the appearance of relaxation processes associated with DNA chain dynamics in the ACFs of solutions containing DNA and oxidized BFDMA (2–20 μM).

Finally, we note that Fig. 4 *a* shows that the sizes of complexes formed between BFDMA and DNA depends strongly on the oxidation state of BFDMA. Because oxidized BFDMA contains three positive charges, whereas reduced BFDMA contains only one positive charge, we reasoned that the change in sizes of the complexes with oxidation state of BFDMA could be a reflection of the change in charge ratio of BFDMA and DNA upon changes in oxidation state of BFDMA. To explore this possibility, we plotted the hydrodynamic sizes of complexes prepared using reduced or oxidized BFDMA as a function of CR (Fig. 4 *b*). We observed that complexes formed using reduced and oxidized BFDMA at the same CR do not result in lipoplexes with comparable sizes. This result suggests that the change in size of the lipoplex as a function of oxidation state of BFDMA is not due solely to a change in charge ratio, but rather reflects a change in the amphiphilic nature of the lipid that occurs upon oxidation of the ferrocene moiety (as described below).

ζ-potentials of complexes of BFDMA and DNA

The ζ-potentials of complexes formed using DNA and BFDMA at concentrations ranging from 2 μM to 100 μM are shown in Fig. 5. The ζ-potentials were negative for lipoplexes prepared using low concentrations of reduced BFDMA (2–8 μM) and transitioned to positive values at high concentrations (20–100 μM), with the change in sign occurring at 10 $\sim\mu$M BFDMA (corresponding to a CR of 1.38). In contrast, the ζ-potentials of complexes formed using oxidized BFDMA were negative over the entire range of concentrations used in this study, with the exception of complexes prepared at 20 μM BFDMA, for which the ζ-potential was close to zero. Fig. 5 *b* shows a plot of the ζ-potentials of complexes prepared using either reduced or oxidized BFDMA as a function of CR. Similar to results obtained by DLS, the lack of correspondence between CR and the ζ-potentials of complexes formed using reduced and oxidized BFDMA suggests that the changes in ζ-potential as a function of oxidation state may be governed by differences

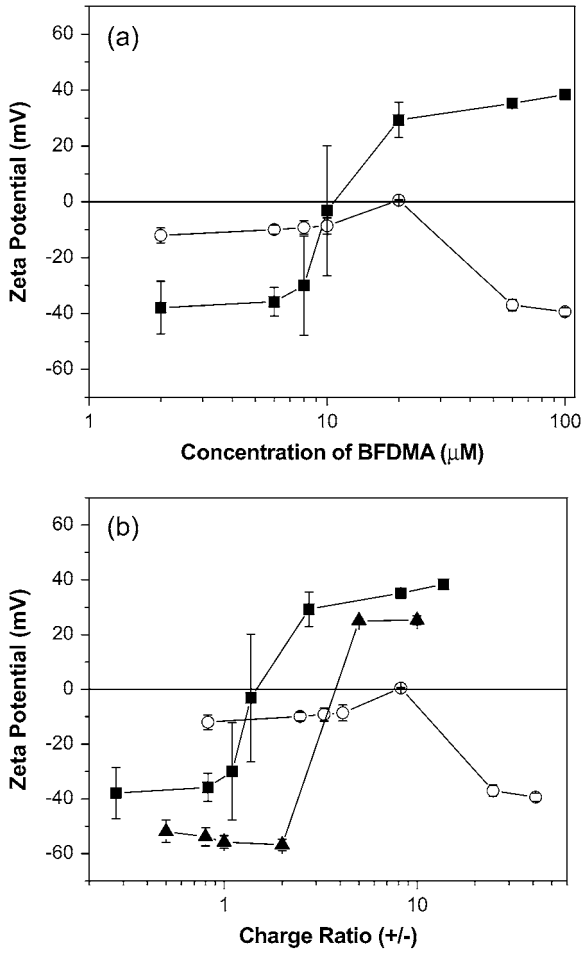

FIGURE 5 ζ-potentials of complexes formed using DNA and lipid (BFDMA or DoDAB/DOPE) in 1 mM Li_2SO_4. (*a*) Plot of ζ-potentials as a function of the concentration of BFDMA and (*b*) plot of ζ-potentials as a function of CR. The symbols correspond to the ζ-potentials of complexes prepared using DNA and reduced BFDMA (■), oxidized BFDMA (○), and DoDAB/DOPE (1:1) (▲).

in the amphiphilicity of reduced and oxidized BFDMA rather than solely by the CR of DNA and BFDMA.

The ζ-potentials of lipoplexes formed using reduced BFDMA as a function of CR are similar to the ζ-potentials of complexes prepared using conventional vesicle-forming cationic lipids (e.g., DoDAB and DOPE, see Fig. 5 *b*), for which monotonic increases in ζ-potentials from at least -30 mV to at least $+30$mV are observed with increasing CR from 0.1 to 10 (22,25,26,30). The observation of negative ζ-potentials for complexes prepared using oxidized BFDMA at high CRs is in striking contrast to the ζ-potentials of lipoplexes formed using reduced BFDMA. The negative ζ-potentials of complexes formed using oxidized BFDMA are similar to past studies of complexes of DNA and spermidine or spermine, in which negative ζ-potentials were reported for CRs up to 50 (42,43). We note that the ζ-potentials of complexes formed by DNA and spermidine (in Tris HCl 3.5 mM, EDTA 0.35 mM, pH 7.6) have been reported to become less negative with increasing CR. We observe the ζ-potential of complexes prepared using oxidized BFDMA to become more negative as the CR increases beyond 8. The negative ζ-potential of complexes formed by oxidized BFDMA and DNA indicate that these complexes possess excess charge due to DNA in their outer regions.

Dynamic light scattering and ζ-potential measurements of lipoplexes in a reduced-serum cell culture medium

The results reported above were obtained by mixing BFDMA and DNA in 1 mM Li_2SO_4, as needed for electrolysis of BFDMA (19,20). For reasons discussed in detail below, here we report measurements of dynamic light scattering and ζ-potentials that were performed using complexes prepared in a reduced-serum cell culture medium (OptiMEM) instead of aqueous Li_2SO_4. OptiMEM is a complex mixture of salts comprising 0.1 M NaCl, 28.6 mM $NaHCO_3$, 5.4 mM KCl, 10 mM HEPES, 1 mM sodium pyruvate and other salts, as well as trace amounts of L-glutamine, hypoxanthine, and thymidine. The motivation for performing these measurements in OptiMEM was twofold. First, we sought to understand the extent to which the above-described conclusions regarding sizes, internal lipoplex dynamics, and ζ-potentials depended on the ionic composition of the solutions. Such an understanding would provide further insights into the importance of electrostatics in determining the structures and properties of the lipoplexes. Second, our past studies investigating the transfection of cells with BFDMA used OptiMEM as a cell culture medium (19,20). Measurements performed in OptiMEM therefore allow us to connect our measurements of dynamic light scattering and ζ-potentials to past measurements that demonstrated the effect of oxidation state of BFDMA on transfection. Below, we summarize the similarities and differences between the dynamic light scattering and ζ-potential measurements performed on complexes prepared using BFDMA and DNA in 1mM Li_2SO_4 and OptiMEM.

We observed the dynamic light scattering behavior of lipoplexes prepared using reduced BFDMA in 1 mM Li_2SO_4 and OptiMEM to be similar in several ways:

1. Angle-dependent light scattering demonstrated that DNA chain dynamics were not evident in the ACFs of lipoplexes prepared using reduced BFDMA in both systems (see Fig. 3, *b* and *e*).
2. The sizes of the lipoplexes formed from reduced BFDMA in both systems passed through a maximum with increasing concentration of BFDMA (Fig. 6 *a*).
3. The sizes of lipoplexes formed from reduced BFDMA in both systems were similar in magnitude (Fig. 6 *a*).

The primary difference between the sizes of the lipoplexes formed using reduced BFDMA in 1 mM Li_2SO_4 versus those prepared in OptiMEM was that the maximum in hydrodynamic size was shifted to a higher concentration of BFDMA when the complexes were prepared in OptiMEM as compared to samples prepared in 1 mM Li_2SO_4, consistent with a

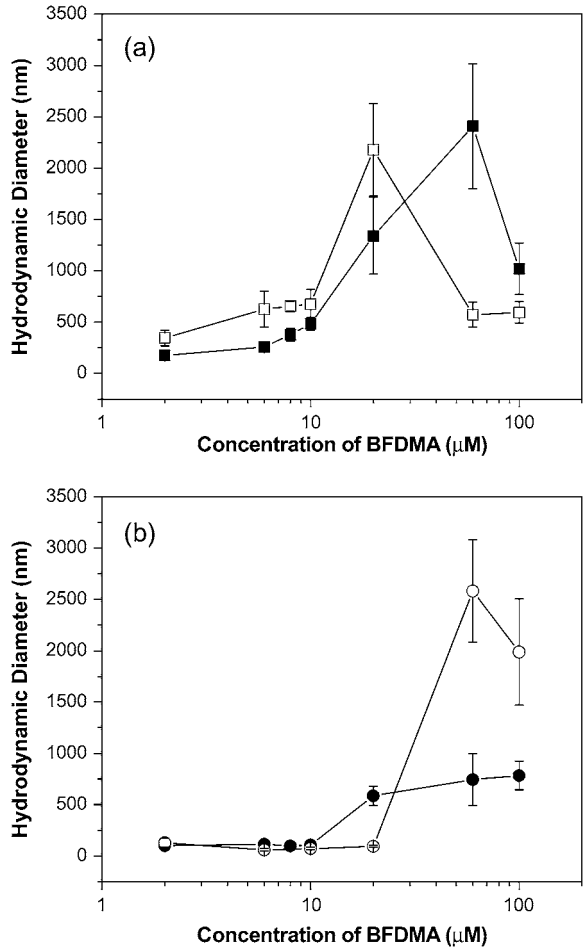

FIGURE 6 Calculated hydrodynamic diameters of complexes formed from reduced and oxidized BFDMA as a function of concentration of BFDMA. (*a*) Lipoplexes formed by reduced BFDMA and DNA in 1 mM Li_2SO_4 (□) and OptiMEM (■). (*b*) Complexes formed by oxidized BFDMA and DNA in 1 mM Li_2SO_4 (○) and OptiMEM (●).

prior study of the sizes of lipoplexes prepared using plasmid DNA and the cationic lipid 1,2-dioleoyl-3-trimethylammonium propane (30).

Inspection of Fig. 6 *b* reveals that the sizes of complexes prepared using DNA and concentrations of oxidized BFDMA ranging from 2 μM to 10 μM are similar when formed in either OptiMEM or 1 mM Li_2SO_4. However, two important differences do exist:

1. The DNA chain dynamics observed in the ACFs of complexes prepared using oxidized BFDMA in 1 mM Li_2SO_4 (Fig. 3 *c*, at concentrations of 2–20 μM) were not present in OptiMEM (Fig. 3 *f*).
2. Complexes prepared at 60–100 μM oxidized BFDMA were substantially larger in 1 mM Li_2SO_4 than they were in OptiMEM.

The ζ-potentials of lipoplexes formed using reduced BFDMA were similar in both 1 mM Li_2SO_4 and OptiMEM (Fig. 5 *a*). The only significant difference between the two systems was the CR at which the sign of the ζ-potential changed from negative to positive, which occurred at a slightly higher concentration of BFDMA in OptiMEM as compared to 1 mM Li_2SO_4. This result is consistent with previous observations reported using lipoplexes prepared using plasmid DNA and various cationic lipids (25,30). The difference between ζ-potentials in OptiMEM and 1 mM Li_2SO_4 is, however, more pronounced for complexes formed by oxidized BFDMA and DNA (Fig. 5 *b*). As the concentration of oxidized BFDMA increases, the ζ-potential of complexes of DNA and oxidized BFDMA formed in 1mM Li_2SO_4 exhibit a maximum in ζ-potential, whereas the ζ-potential becomes less negative for complexes formed in OptiMEM. We note that the increase in ζ-potential to nearly zero as a function of CR for complexes prepared in OptiMEM is similar to past studies of the ζ-potential of complexes of DNA and either spermidine or spermine performed in 3.5 mM and 10 mM Tris HCl, respectively (42,43). We return to these observations in the discussion below.

DISCUSSION

This article describes measurements of dynamic light scattering and ζ-potential of complexes formed between DNA and a ferrocene-containing, cationic lipid (BFDMA) as a function of concentration and oxidation state of the lipid, and the complexity of the ionic environment (1mM Li_2SO_4 versus OptiMEM). Our measurements of lipoplexes formed using reduced BFDMA suggest a physical situation that is similar to that of lipoplexes formed using classical cationic lipids such as DoDAB mixed with DOPE (26,30). Our measurements of these lipoplexes (formed using reduced BFDMA or DoDAB/DOPE) reveal that as the CR is increased, the hydrodynamic size passes through a maximum and the ζ-potential changes sign from negative to positive (Figs. 4 *b* and 5 *b*). These two phenomena are linked, and reflect the compensation and then overcompensation of the charges of DNA by the cationic lipid with increasing concentration of lipid (4,7,9,22,24). These observations are consistent with those expected for complexes formed by DNA and self-associating cationic lipids (4,21,23,64) or cationic polyelectrolytes (65,66). In this respect, the tendency of reduced BFDMA to self-associate into large vesicle-like aggregates underlies the trends observed in both size and ζ-potential. This physical picture, in which the DNA is constrained within a structured aggregate of BFDMA, is consistent with the absence of internal DNA chain dynamics in the ACFs of samples prepared from DNA and reduced BFDMA (Fig. 3 *b*). Past studies of lipoplexes of DNA and cationic lipids have also determined that the amphiphilic nature of the lipids leads to organized microstructures within the lipoplex, including lamellar and hexagonal ordering, in which the DNA is confined within an organized lipid assembly (5,7,31,32). The similarity between the behavior of reduced BFDMA and conventional cationic lipids is reinforced by the similar effects of the ionic environment (1 mM Li_2SO_4 versus OptiMEM) on the hydrodynamic sizes and ζ-potentials of the lipoplexes (Figs. 6 *a* and 7 *a*) (25, 30).

In contrast to lipoplexes formed using reduced BFDMA, the change in the sizes of the complexes formed by DNA and oxidized BFDMA as a function of the concentration of oxidized BFDMA is not similar to the behavior discussed above for lipoplexes formed from conventional cationic lipids (4,21,24,26). With increasing charge ratio, we observed a minimum in the hydrodynamic sizes of complexes formed using oxidized BFDMA in 1 mM Li_2SO_4 (Fig. 4 and Table 1), which is similar to the behavior observed for complexes of DNA and non-self-associating molecules that possess multiple positive charges (e.g., spermidine) (34–41). This result suggests that the reduced amphiphilicity of oxidized BFDMA plays a central role in determining the structure and properties of complexes formed by oxidized BFDMA and DNA.

Our measurements yield two additional insights into the nature of the complexes formed between oxidized BFDMA and DNA. First, the ACFs obtained from light scattering measurements using solutions of DNA and 2–20 μM oxidized BFDMA revealed contributions to the ACFs that we attribute to the motions of DNA chains within the complexes (Fig. 3 *c*) (57,58). Similar dynamics were evident in solutions containing DNA in the absence of BFDMA (Fig. 3 *a*), but not in solutions of lipoplexes prepared using reduced BFDMA (Fig. 3 *b*). This result suggests a physical picture of the complexes formed using oxidized BFDMA in which the complexes are loosely packed and/or disordered, thus providing DNA chains with substantial conformational freedom. The negative values of the ζ-potentials of these complexes (Fig. 5) also suggest that the net charges of the outermost regions of these complexes are dominated by contributions from DNA. A second key observation is that the sizes and ζ-potentials of the complexes formed using oxidized BFDMA

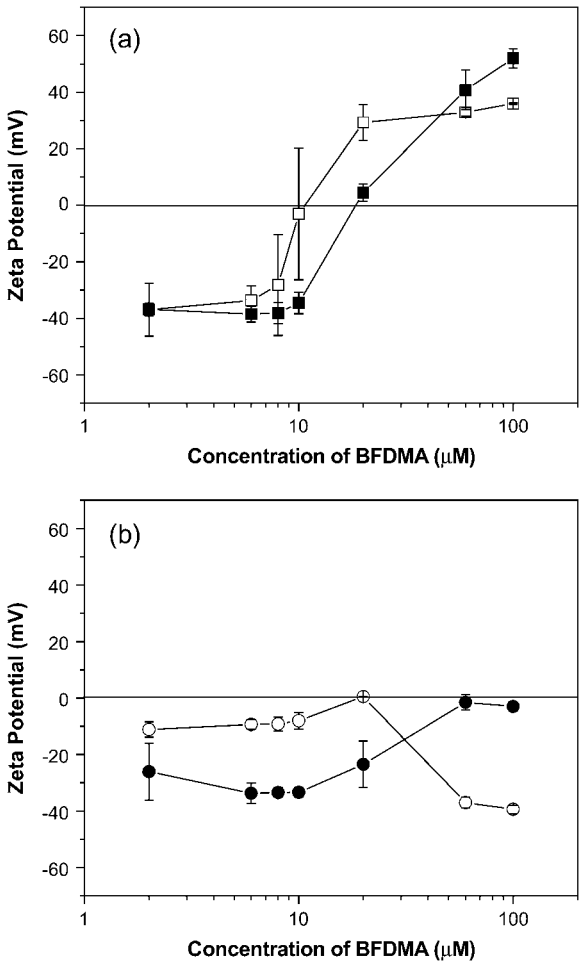

FIGURE 7 ζ-potentials of complexes formed from reduced and oxidized BFDMA as a function of concentration of BFDMA. (*a*) Lipoplexes formed by reduced BFDMA and DNA in 1 mM Li_2SO_4 (□) and OptiMEM (■). (*b*) Complexes formed by oxidized BFDMA and DNA in 1 mM Li_2SO_4 (○) and OptiMEM (●).

are influenced by the change from 1 mM Li_2SO_4 to OptiMEM (Figs. 6 *b* and 7 *b*) to an extent that is much greater than lipoplexes formed using reduced BFDMA (Figs. 6 *a* and 7 *a*), particularly at CRs greater than unity. These results are consistent with the physical picture described above, in which loosely packed and/or disordered complexes prepared using oxidized BFDMA are held together largely by a network of electrostatic interactions that are perturbed by the higher ionic strength of OptiMEM. In contrast, lipoplexes formed using reduced BFDMA are strongly influenced by the amphiphilicity of reduced BFDMA and form well-ordered structures that are not substantially disrupted upon a change in ionic strength of the solution.

The results discussed above reveal that the physical properties of complexes formed between DNA and BFDMA change substantially with the oxidation state of BFDMA. The oxidation state-dependent properties of the complexes formed by BFDMA and DNA that we have identified include the size (Fig. 4), internal dynamics (Fig. 3), and ζ-potential (Fig. 5). The hydrodynamic sizes of lipoplexes prepared using reduced BFDMA in the concentration range that gave the highest levels of cell transfection in our past studies (6–20 μM) (19) were >200 nm when measured in OptiMEM (lipoplexes at 20 μM were larger than 1 μm; see Fig. 6 *a*). These sizes are larger than the sizes generally considered to be optimal for the internalization of DNA by endocytosis (4,23,27,28). It is possible, however, that a small subpopulation of lipoplexes with diameters <200 nm is responsible for the efficient transfection observed in these past studies. In contrast, the hydrodynamic sizes of complexes formed using 6–10 μM oxidized BFDMA were 50 nm (Fig. 6 *b*), which is small enough for endocytosis. We note, however, that high levels of transfection were not observed using these complexes in our earlier studies (19). Furthermore, the observation of a change in the internal dynamics of DNA in BFDMA-DNA complexes with a change in oxidation state of BFDMA hints at differences in the structures of these complexes. These differences in internal dynamics, however, were not observed in OptiMEM (Fig. 3, *e* and *f*). Independent measurements of the microstructures of the complexes formed by DNA and BFDMA by electron microscopy and neutron scattering are ongoing and will be reported in a future publication.

Perhaps the most significant result of the study reported in this article is that the ζ-potentials of complexes formed between DNA and either oxidized or reduced BFDMA differed significantly (Figs. 5 and 7). Specifically, the ζ-potentials of lipoplexes formed using reduced BFDMA changed sign (from negative to positive) as the concentration of BFDMA was increased from 6 μM to 20 μM (Fig. 5 *a*), whereas the ζ-potentials of complexes formed using oxidized BFDMA were negative over this same concentration range (Fig. 5 *b*). This result could be significant in the understanding of the dependence of transfection on the oxidation state of BFDMA observed in our previous studies (19) because positive ζ-potentials often correlate with effective cell transfection, likely due to the nonspecific electrostatic attractions between negatively-charged cell membranes and positively-charged lipoplexes (22,25,30). These results lead to the proposition that the strong dependence of transfection efficiency on the oxidation state of BFDMA, as reported previously, is largely a reflection of the substantial change in the ζ-potentials of these complexes with changes in the oxidation state of BFDMA (and is less likely to be a consequence of other factors such as changes in sizes of lipoplexes with oxidation state of BFDMA).

CONCLUSIONS

Measurements of dynamic light scattering and ζ-potentials of complexes formed by DNA and BFDMA reveal a strong dependence on the oxidation state of BFDMA. The sizes, ζ-potentials, and internal DNA chain dynamics (or absence

thereof) of complexes formed by reduced BFDMA and DNA are very similar to those reported for lipoplexes formed by DNA and classical cationic lipids. In contrast, the properties of complexes formed by oxidized BFDMA and DNA differ significantly from those of lipoplexes of cationic lipids and DNA, and are more closely identified with the properties of complexes typically formed by DNA and cationic molecules that possess multiple charges but do not self-associate (e.g., spermidine). In particular, the complexes formed by oxidized BFDMA and DNA appear to be loosely packed (as evidenced by contributions to light scattering by internal DNA chain dynamics) and possess coronas with net negative charges. These results suggest that the properties of complexes formed by DNA and either reduced or oxidized BFDMA can be understood in terms of a change in the amphiphilicity of BFDMA (i.e., tendency to self-associate) upon oxidation of ferrocene. Our results also suggest that the substantial changes in ζ-potentials that accompany changes in the oxidation state of the BFDMA may underlie the previously reported dependence of transfection efficiency on the oxidation state of BFDMA.

SUPPLEMENTARY MATERIAL

To view all of the supplemental files associated with this article, visit www.biophysj.org.

Financial support was provided by the National Science Foundation (grants Nos. CTS-0327489, CTS-0553760, and DMR-0520527), the Arnold and Mabel Beckman Foundation, and the National Institutes of Health (grant No. R21 EB02746).

REFERENCES

1. Felgner, P. L., T. R. Gadek, M. Holm, R. Roman, H. W. Chan, M. Wenz, J. P. Northrop, G. M. Ringold, and M. Danielsen. 1987. Lipofection: a highly efficient, lipid-mediated DNA-transfection procedure. *Proc. Natl. Acad. Sci. USA.* 84:7413–7417.
2. Huang, L., M.-C. Hung, and E. Wagner. 1999. Nonviral Vectors for Gene Therapy. Academic Press, San Diego, CA.
3. Felgner, P. L., Y. J. Tsai, L. Sukhu, C. J. Wheeler, M. Manthorpe, J. Marshall, and S. H. Cheng. 1995. Improved cationic lipid formulations for in vivo gene therapy. *Ann. N. Y. Acad. Sci.* 772:126–139.
4. Miller, A. D. 1998. Cationic liposomes for gene therapy. *Angew. Chem. Int. Ed. Engl.* 37:1768–1785.
5. Safinya, C. R. 2001. Structures of lipid-DNA complexes: supramolecular assembly and gene delivery. *Curr. Opin. Struct. Biol.* 11:440–448.
6. Remy, J., B. Abdallah, M. Zanta, O. Boussif, J. Behr, and B. Demeneix. 1998. Gene transfer with lipospermines and polyethylenimines. *Adv. Drug Deliv. Rev.* 30:85–95.
7. Schatzlein, A. G. 2001. Non-viral vectors in cancer gene therapy: principles and progress. *Anticancer Drugs.* 12:275–304.
8. Weithoff, C., and C. R. Middaugh. 2003. Barriers to nonviral gene delivery. *J. Pharm. Sci.* 92:203–217.
9. Zabner, J. 1997. Cationic lipids used in gene transfer. *Adv. Drug Deliv. Rev.* 27:17–28.
10. Zabner, J., A. J. Fasbender, T. Moninger, K. A. Poellinger, and M. J. Welsh. 1995. Cellular and molecular barriers to gene transfer by a cationic lipid. *J. Biol. Chem.* 270:18997–19007.
11. Martin, B., M. Sainlos, A. Aissaoui, N. Oudrhiri, M. Hauchecorne, J.-P. Vigneron, J.-M. Lehn, and P. Lehn. 2005. The design of cationic lipids for gene delivery. *Curr. Pharm. Des.* 11:375–394.
12. Hirko, A., F. Tang, and J. A. Hughes. 2003. Cationic lipid vectors for plasmid DNA delivery. *Curr. Med. Chem.* 10:1185–1196.
13. Guo, X., and F. C. Szoka. 2003. Chemical approaches to triggerable lipid vesicles for drug and gene delivery. *Acc. Chem. Res.* 36:335–341.
14. Prata, C. A. H., Y. X. Zhao, P. Barthelemy, Y. G. Li, D. Luo, T. J. McIntosh, S. J. Lee, and M. W. Grinstaff. 2004. Charge-reversal amphiphiles for gene delivery. *J. Am. Chem. Soc.* 126:12196–12197.
15. Meers, P. 2001. Enzyme-activated targeting of liposomes. *Adv. Drug Deliv. Rev.* 53:265–272.
16. Kakizawa, Y., H. Sakai, A. Yamaguchi, Y. Kondo, N. Yoshino, and M. Abe. 2001. Electrochemical control of vesicle formation with a double-tailed cationic surfactant bearing ferrocenyl moieties. *Langmuir.* 17: 8044–8048.
17. Kakizawa, Y., H. Sakai, K. Nishiyama, M. Abe, H. Shoji, Y. Kondo, and N. Yoshino. 1996. Solution properties of double-tailed cationic surfactants having ferrocenyl groups in their hydrophobic moieties. *Langmuir.* 12:921–924.
18. Yoshino, N., H. Shoji, Y. Kondo, Y. Kakizawa, H. Sakai, and M. Abe. 1996. Syntheses of cationic surfactants having two ferrocenylalkyl chains. *J. Japan. Oil Chem. Soc.* 45:769–775.
19. Jewell, C. M., M. E. Hays, Y. Kondo, N. L. Abbott, and D. M. Lynn. 2006. Ferrocene-containing cationic lipids for the delivery of DNA: oxidation state determines transfection activity. *J. Controlled Release.* 112:129–138.
20. Abbott, N. L., C. M. Jewell, M. E. Hays, Y. Kondo, and D. M. Lynn. 2005. Ferrocene-containing cationic lipids: influence of redox state on cell transfection. *J. Am. Chem. Soc.* 127:11576–11577.
21. Chesnoy, S., and L. Huang. 2000. Structure and function of lipid-DNA complexes for gene delivery. *Annu. Rev. Biophys. Biomol. Struct.* 29: 27–47.
22. Tomlinson, E., and A. P. Rolland. 1996. Controllable gene therapy. Pharmaceutics of non-viral gene delivery systems. *J. Controlled Release.* 39:357–372.
23. Hope, M. J., B. Mui, S. Ansell, and Q. F. Ahkong. 1998. Cationic lipids, phosphatidylethanolamine and the intracellular delivery of polymeric, nucleic acid-based drugs (Review). *Mol. Membr. Biol.* 15: 1–14.
24. Zuhorn, I. S., and D. Hoekstra. 2002. On the mechanism of cationic amphiphile-mediated transfection. To fuse or not to fuse: is that the question? *J. Membr. Biol.* 189:167–179.
25. Eastman, S. J., C. Siegel, J. Tousignant, A. E. Smith, S. H. Cheng, and R. K. Scheule. 1997. Biophysical characterization of cationic lipid: DNA complexes. *Biochim. Biophys. Acta.* 1325:41–62.
26. Birchall, J. C., I. W. Kellaway, and S. N. Mills. 1999. Physico-chemical characterisation and transfection efficiency of lipid-based gene delivery complexes. *Int. J. Pharm.* 183:195–207.
27. Vijayanathan, V., T. Thomas, and T. J. Thomas. 2002. DNA nanoparticles and development of DNA delivery vehicles for gene therapy. *Biochemistry.* 41:14085–14094.
28. Zhdanov, R. I., O. V. Podobed, and V. V. Vlassov. 2002. Cationic lipid-DNA complexes–lipoplexes for gene transfer and therapy. *Bioelectrochemistry.* 58:53–64.
29. Almofti, M. R., H. Harashima, Y. Shinohara, A. Almofti, Y. Baba, and H. Kiwada. 2003. Cationic liposome-mediated gene delivery: biophysical study and mechanism of internalization. *Arch. Biochem. Biophys.* 410:246–253.
30. Lobo, B. A., A. Davis, G. Koe, J. G. Smith, and C. R. Middaugh. 2001. Isothermal titration calorimetric analysis of the interaction between cationic lipids and plasmid DNA. *Arch. Biochem. Biophys.* 386:95–105.
31. Koltover, I., T. Salditt, J. O. Radler, and C. R. Safinya. 1998. An inverted hexagonal phase of cationic liposome-DNA complexes related to DNA release and delivery. *Science.* 281:78–81.

32. Alfredsson, V. 2005. Cryo-TEM studies of DNA and DNA-lipid structures. *Curr. Opin. Colloid Interface Sci.* 10:269–273.
33. Koynova, R., H. S. Rosenzweig, L. Wang, M. Wasielewski, and R. C. MacDonald. 2004. Novel fluorescent cationic phospholipid, O-4-naphthylimido-1-butyl-DOPC, exhibits unusual foam morphology, forms hexagonal and cubic phases in mixtures, and transfects DNA. *Chem. Phys. Lipids.* 129:183–194.
34. He, S., P. G. Arscott, and V. A. Bloomfield. 2000. Condensation of DNA by multivalent cations: experimental studies of condensation kinetics. *Biopolymers.* 53:329–341.
35. Deng, H., and V. A. Bloomfield. 1999. Structural effects of cobalt-amine compounds on DNA condensation. *Biophys. J.* 77:1556–1561.
36. Patel, M. M., and T. J. Anchordoquy. 2005. Contribution of hydrophobicity to thermodynamics of ligand-DNA binding and DNA collapse. *Biophys. J.* 88:2089–2103.
37. Conwell, C. C., and N. V. Hud. 2004. Evidence that both kinetic and thermodynamic factors govern DNA toroid dimensions: effects of magnesium (II) on DNA condensation by hexamine cobalt (III). *Biochemistry.* 43:5380–5387.
38. Khan, M. O., and B. Jonsson. 1999. Electrostatic correlations fold DNA. *Biopolymers.* 19:121–125.
39. Widom, J., and R. L. Baldwin. 1980. Cation-induced toroidal condensation of DNA studies with $Co^{3+}(NH_3)^6$. *J. Mol. Biol.* 144:431–453.
40. Wilson, R. W., and V. A. Bloomfield. 1979. Counterion-induced condensation of deoxyribonucleic acid. A light-scattering study. *Biochemistry.* 18:2192–2196.
41. Sen, D., and D. M. Crothers. 1986. Condensation of chromatin: role of multivalent cations. *Biochemistry.* 25:1495–1503.
42. de Frutos, M., E. Raspaud, A. Leforestier, and F. Livolant. 2001. Aggregation of nucleosomes by divalent cations. *Biophys. J.* 81:1127–1132.
43. Raspaud, E., I. Chaperon, A. Leforestier, and F. Livolant. 1999. Spermine-induced aggregation of DNA, nucleosome, and chromatin. *Biophys. J.* 77:1547–1555.
44. Sternberg, B., K. Hong, W. Zheng, and D. Papahadjopoulos. 2000. Optimization of cationic liposome/DNA complexes for in vivo applications: correlation between transfection activity and morphology. NATO Science Series, Series A. *Life Sci.* 323:156–164.
45. Xu, Y., and F. C. J. Szoka. 1996. Mechanism of DNA release from cationic liposome/DNA complexes used in cell transfection. *Biochemistry.* 35:5616–5623.
46. Barreleiro, P. C. A., R. P. May, and B. Lindman. 2002. Mechanism of formation of DNA-cationic vesicle complexes. *Faraday Discuss.* 122: 191–201.
47. Provencher, S. W. 1982. A constrained regularization method for inverting data represented by linear algebraic or integral equations. *Comput. Phys. Commun.* 27:213–227.
48. Provencher, S. W. 1982. CONTIN: a general purpose constrained regularization program for inverting noisy linear algebraic and integral equations. *Comput. Phys. Commun.* 27:229–242.
49. Porsch, B., S. Nilsson, and L. O. Sundelof. 1997. Association of ethyl(hydroxyethyl)cellulose solutions. *Macromolecules.* 30:4626–4632.
50. Chu, B. 1991. Laser Light Scattering: Basic Principles and Practice, 2nd Ed. Academic Press, Boston, MA.
51. Kjoniksen, A. L., B. Nystrom, and B. Lindman. 1998. Effects of temperature, surfactant concentration, and salinity of the dynamics of dilute solutions of a nonionic cellulose derivative. *Langmuir.* 14:5039–5045.
52. Nystrom, B., K. Thuresson, and B. Lindman. 1995. Rheological and dynamic light-scattering-studies on aqueous solutions of a hydrophobically modified nonionic cellulose ether and its unmodified analog. *Langmuir.* 11:1994–2002.
53. Hays, M. E., and N. L. Abbott. 2005. Electrochemical control of the interactions of polymers and redox-active surfactants. *Langmuir.* 21:12007–12015.
54. Douglas, J. F., and J. B. Hubbard. 1991. Semiempirical theory of relaxation—concentrated polymer- solution dynamics. *Macromolecules.* 24:3163–3177.
55. Wang, C. H. 1992. Dynamic light scattering and linear viscoelasticity of polymers in solution and in the bulk. *In* Dynamic Light Scattering. The Method and Some Applications. W. Brown, Editor. Oxford Press, Oxford, UK.
56. Hunter, R. J. 1981. Zeta Potential in Colloid Science. Academic Press, New York, NY.
57. Sorlie, S. S., and R. Pecora. 1988. A dynamic light scattering study of a 2311 base pair DNA restriction fragment. *Macromolecules.* 21:1437–1449.
58. Sorlie, S. S., and R. Pecora. 1990. A dynamic light scattering study of four DNA restriction fragments. *Macromolecules.* 23:487–497.
59. Choosakoonkriang, S., C. M. Wiethoff, T. J. Anchordoquy, G. S. Koe, J. G. Smith, and C. R. Middaugh. 2001. Infrared spectroscopic characterization of the interaction of cationic lipids with plasmid DNA. *J. Biol. Chem.* 276:8037–8043.
60. Ferrari, M. E., D. Rusalov, J. Enas, and C. J. Wheeler. 2001. Trends in lipoplex physical properties dependent on cationic lipid structure, vehicle and complexation procedure do not correlate with biological activity. *Nucleic Acids Res.* 29:1539–1548.
61. Xu, Y., S.-W. Hui, P. Frederik, and F. C. Szoka, Jr. 1999. Physicochemical characterization and purification of cationic lipoplexes. *Biophys. J.* 77:341–353.
62. You, J., M. Kamihira, and S. Iijima. 1997. Surfactant-mediated gene transfer for animal cells. *Cytotechnology.* 25:45–52.
63. Langowski, J., and U. Geisen. 1989. Configurational and dynamic properties of different length superhelical DNAs measured by dynamic light scattering. *Biophys. Chem.* 34:9–18.
64. Felgner, P. L. 1996. Artificial self-assembling systems for gene delivery. Conference Proceedings Series, Vol. 200. American Chemical Society, Washington, DC.
65. Pack, D. W., A. S. Hoffman, S. Pun, and P. S. Stayton. 2005. Design and development of polymers for gene delivery. *Nat. Rev. Drug Discov.* 4:581–593.
66. Luo, D., and W. M. Saltzman. 2000. Synthetic DNA delivery systems. *Nat. Biotechnol.* 18:33–37.